# In-situ synthesis of a ZrB$_2$–based composite powder using a mechanochemical reaction for the zircon/magnesium/boron oxide/graphite system

M. Jalaly [1,*], M.Sh. Bafghi [1], M. Tamizifar [1], F.J. Gotor [2]

1. School of Metallurgy and Materials Engineering, Iran University of Science & Technology (IUST), Narmak, Tehran 16846-13114, Iran

2. Instituto de Ciencia de Materiales de Sevilla (CSIC-US), Americo Vespucio 49, 41092 Sevilla, Spain

*Corresponding Author, Email: maisam_jalaly@iust.ac.ir

Tel: +989127387902, Fax: +982177240480

## Abstract

A ZrSiO$_4$/B$_2$O$_3$/Mg/C system was used to synthesize a ZrB$_2$-based composite through a high energy ball milling process. As a result of the milling process, a mechanically induced self-sustaining reaction (MSR) was achieved in this system. A composite powder of ZrB$_2$–SiC–ZrC was prepared in-situ by a magnesiothermic reduction with an ignition time of approximately 6 minutes. The mechanism for the formation of the product was investigated by studying the relevant sub-reactions, the stoichiometric amount of B$_2$O$_3$ and thermal analysis.

**Keywords:** Ceramic; Composites; Chemical Synthesis; X-ray diffraction;

## 1. Introduction

ZrB$_2$ exhibits a number of excellent properties including a high melting point (3245°C), high hardness (23 GPa), high electrical conductivity ($10^7$ S/m) and thermal

conductivity (~60 W/mK), superb thermal resistance and chemical inertness [1]. For these reason, $ZrB_2$ is expected to be one of the most promising materials for use in high-temperature applications. However, $ZrB_2$ is difficult to sinter, and $ZrB_2$ alone does not meet all of the necessary requirements for use in aerospace engineering applications, especially oxidation resistance [1, 2]. Consequently, $ZrB_2$ is usually employed in a composite mode with other refractory ceramics.

SiC is one of the most widely used materials for creating a composite containing $ZrB_2$ [3-6]. SiC enhances sinterability, oxidation resistance and mechanical properties of zirconium diboride [7]. Several researchers have studied the use of other ceramic compounds, such as ZrC [8], $MoSi_2$ [9, 10], AlN [11] and $TiB_2$ [12], in binary or ternary composites. Various methods have been used to synthesize $ZrB_2$-based composites. For example, ternary composite of $ZrB_2$–SiC–ZrC have been fabricated using a variety of methods such as spark plasma sintering of blended compounds [13, 14], the induction of reactions in the $Zr/Si/B_4C$ system during heating followed by hot pressing [15] and reactive hot pressing of the $Zr/Si/B_4C$ system [16].

However, a literature survey shows a strong tendency towards the use of aluminum and magnesium in reduction of $ZrO_2$ and $B_2O_3$ for preparing $ZrB_2$. Such approaches take advantages of more affordable raw materials, compared with other synthesis mechanisms, as well as the highly exothermic nature of the these reactions enabling the use of self-propagating (or self-sustaining) processes [17-22]. The self-sustaining reaction caused by high energy ball milling of reactants for a critical milling period, called the ignition time, is a mechanochemical process referred to as a mechanically induced self-sustaining reaction (MSR). In contrast to the conventional self-propagating high-temperature synthesis (SHS), an MSR process has the favorable

side benefits of mixing of the reactants, the homogenization of the products and an intensive reduction of particle size in one single step.

Zircon ($ZrSiO_4$), as a single source for both zirconium and silicon, may be employed for the synthesis of $ZrB_2$–SiC-based composites, which has not been used widely so far. The aim of the present work, therefore, was to investigate the magnesiothermic reduction of $ZrSiO_4$ and $B_2O_3$ for the in-situ preparation of the $ZrB_2$–SiC-based composite powder by means of an MSR process. Additionally, this work aims to explain the mechanism of the formation of $ZrB_2$-based materials in this system by studying sub-reactions as well as the influence of stoichiometry of the reactants.

## 2. Experimental

The raw materials used in this work were $ZrSiO_4$ (98%, Alfa-Aesar, USA), $B_2O_3$ (98%, Fluka, USA), graphite (99%, Fluka, USA) and Mg (99%, Riedel-deHaen, Germany). The particle sizes of all starting powders were in the range of 5-10 micrometer. The initial materials were subjected to high energy dry ball milling in a modified planetary ball mill (Pulverisette7, Fritsch, Germany). The rotational speed and ball-to-powder mass ratio were 600 rpm and 30:1, respectively. The milling vial and balls (15 mm) were made of hardened chromium steel. All milling experiments were conducted under high purity argon gas at a constant pressure of 5 bar. Before the start of the milling, the vial was purged with argon gas several times, and the desired pressure was finally adjusted. The connection of the vial to the gas cylinder during the milling experiments was maintained by a rotating union and a flexible polyamide tube. The internal pressure of the vial was monitored by an SMC solenoid valve (model EVT307-5DO-01F-Q, SMC Co,. Tokyo, Japan) to determine the ignition time. A sharp peak due

to the pressure rise appears in the pressure-time record when the self-sustaining reaction occurs as a result of the heat generated. The position of this peak determines the ignition time. The system used in this work has been previously presented elsewhere [23]. The magnesium oxide by-product was eliminated by leaching the as-milled powder in 1M HCl at 80°C for 1h. The ZrB$_2$-based composite was then reclaimed by a centrifuge machine with a rotational speed of 15000 rpm for 20 min.

The general web-site [24] of FactSage software was used to obtain thermodynamic data. The adiabatic temperature (T$_{ad}$) values were calculated using following equation:

$$Q = (-\Delta H^{\circ}_{298}) = \int_{298}^{T_{ad}} \Sigma \, C_p (\text{Products}) dT \qquad (1)$$

where $Q$ is the heat of reaction, $\Delta H^{\circ}_{298}$ is the standard enthalpy change at room temperature and $C_p$ is the heat capacity of products.

The structural features of the samples were investigated using X-ray powder diffraction (XRD) analysis with a Panalitycal X'Pert diffractometer (45 kV, 40 mA) using Cu Kα radiation (λ=0.15406 nm). Thermal specifications of powder mixtures were studied by differential scanning calorimetry (DSC) using a TA Instrument Q600 with a constant heating rate of 10°C/min. The DSC measurements were performed in a flowing helium atmosphere. Furthermore, isothermal annealing of powders was carried out at different temperatures in a horizontal tubular furnace (IGM1360 model no. RTH-180-50-1H, AGNI) with a dwell time of 30 min under a flowing argon atmosphere at a pressure of 1 bar.

## 3. Results and Discussion

### 3.1. Mechanosynthesis

The first objective of the work was to synthesize a zirconium diboride–silicon carbide-based composite from a $ZrSiO_4$, $B_2O_3$, Mg and C mixture. To achieve this goal, the main reaction required is described by the following equation:

$$ZrSiO_4 + B_2O_3 + 7Mg + C \rightarrow ZrB_2 + SiC + 7MgO \qquad (2)$$
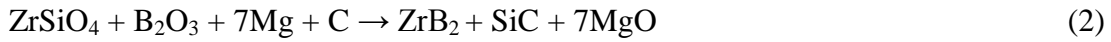
$\Delta G°_{298} = -1270$ kJ,  $\Delta H°_{298} = -1300$ kJ,  $T_{ad} \approx 2750$ K

This reaction possesses the necessary conditions to satisfy Merzhanov criterion (adiabatic temperature, $T_{ad} > 1800$ K [25]) for a self-sustaining reaction. Stoichiometric amounts of the initial materials were milled under the previously described experimental conditions. As seen in Fig. 1, a large pressure rise was observed in the diagram of internal pressure of the vial versus milling time, which corresponds to an intense exothermic reaction with a short ignition time of 6 min. Similar ignition time was observed by the authors during the magnesiothermic reductive mechanosynthesis of zirconium diboride from $ZrO_2$ and $B_2O_3$ [26]. Some research has already used magnesium for the synthesis of $ZrB_2$ from $ZrO_2$ and $B_2O_3$ through high energy milling. The ignition time in this study and also our previous work [26] was 6 min while $ZrB_2$ has been reported in other works to be prepared within longer times, for example 15 [19] and 30 [21] hours of milling. The preparation in longer times indicates that no MSR ignitions in those past studies have occurred. The main difference between the present research and other works lies in the milling intensity (rotational speed of 600 rpm used in our works as compared to values of 165 rpm [19] and 300 rpm [21] in other works), thus providing an example of the critical role that the milling conditions play in the development of a self-sustaining reaction.

Figure 2 shows the XRD patterns of $ZrSiO_4$, $B_2O_3$, C and Mg powder mixture as-blended and after different milling times. The XRD pattern of the as-blended mixture

shows only the sharp peaks from the initial materials. The XRD pattern in Fig. 2 of the sample taken immediately after ignition (6 min of milling) clearly shows the production of $ZrB_2$ as the major phase together with MgO, SiC and ZrC. A negligible amount of $Mg_2SiO_4$ was also detected. A slight amount of $ZrSiO_4$ remained in the mixture immediately after ignition, which is typical behavior in mechanosynthesis reactions, especially for MSR reactions [27] that occur over short time periods. This result is due to incomplete mixing of reactants in a short time and the entrapment of some powders in the dead zones of the milling vial. By increasing the milling time, these trapped powders will gradually be exposed to the ball impacts and will be locally reacted. Figure 2 shows the XRD pattern of a sample milled for 3 h in which the remaining $ZrSiO_4$ and $Mg_2SiO_4$ phases disappeared entirely. Dissolution of the MgO by-product was carried out by using a 1M HCl solution. The XRD pattern of leached product after 3 h of milling is shown in Fig. 2. The MgO has been completely removed, and the of $ZrB_2$–SiC–ZrC composite product remained.

## 3.2. Mechanism of product formation

### 3.2.1. Milling process

As shown in Fig. 2, ZrC was not initially considered in reaction *(2)* but is clearly an observed compound in this system. ZrC can also be considered as a beneficial by-product. The formation of products that include ZrC may be explained by the following reaction mechanism. Zircon and boron oxide must be reduced to their corresponding elements to form the target compounds. These sub-reactions are as follows:

$$3Mg + B_2O_3 \rightarrow 2B + 3MgO \tag{3}$$

$\Delta G°_{298} = -515$ kJ,  $\Delta H°_{298} = -532$ kJ,  $T_{ad} \approx 2630$ K

$$4Mg + ZrSiO_4 + C \rightarrow Zr + Si + C + 4MgO \qquad\qquad (4)$$

$\Delta G^{\circ}_{298} = -363$ kJ,  $\Delta H^{\circ}_{298} = -377$ kJ,  $T_{ad} \approx 1575$ K

Regarding the adiabatic temperatures ($T_{ad}$) and enthalpy values of the above reactions, reaction *(3)* satisfies the Merzhanov criterion to proceed in a self-sustaining manner. However, the reduction of $ZrSiO_4$ by Mg (reaction *4*) does not satisfy this condition, and hence is expected to be a gradual solid state ordinary reaction. If reaction *(4)* occurs, the Zr, Si and C may form ZrC and SiC compounds in a subsequent step, which actually happened in overall reaction as Fig. 2 shows. Zirconium disilicide cannot form as discussed below.

However, when the Mg, $B_2O_3$ and $ZrSiO_4$ are simultaneously present in a system, the stoichimetric fraction of Mg is able to reduce $B_2O_3$ in a self-sustaining manner to yield elemental B and MgO together with the release of a significant amount of heat. Such a heat release increases the instantaneous temperature inside the milling vial to a level that can trigger the reaction between Mg and $ZrSiO_4$ to form elemental Zr and Si.

The presence of the spinel phase of $Mg_2SiO_4$ among products just after ignition may be an indication of an intermediate step in which $ZrSiO_4$ first decomposes to its individual oxides, $ZrO_2$ and $SiO_2$, due to the heat generated by the reduction of boron oxide. At the same time, a slight amount of silicon oxide combines with some of the produced MgO to form magnesium silicate. The $ZrO_2$ and $SiO_2$ are subsequently reduced by the remainder of magnesium to form elemental silicon and zirconium. Figure 3 shows the changes of gibbs free energy of zircon decomposition versus temperature. It can be seen that greater than 1850 K, zircon is thermodynamically possible to decompose to its individual oxides. When ignition occurs in the reaction *(2)*, the temperature of the system increases theoretically to the adiabatic temperature (2750

K), which is greatly larger than 1850 K. Thus, decomposition of zircon in the ignition moment is justifiable.

Therefore, after both the reduction reactions, elemental Si, Zr, B and C are present in the system. Figure 4 shows the standard free energy of the formation of various possible compounds that may be created from these elements. $ZrB_2$ clearly has the most negative energy; hence, boron has the highest tendency to react with zirconium to form zirconium diboride. The highly exothermic formation reaction of $ZrB_2$ may provide extra heat to the system, which allows the $ZrSiO_4$ reduction reaction to proceed more easily and avoids extinction of the self-sustaining reaction. In spite of $ZrB_2$, Fig. 4 shows a fairly high tendency for the formation of ZrC compared to the other compounds, especially $ZrSi_2$. Therefore, it appears reasonable that ZrC is formed by the reaction of some of the Zr and C present in the system. Finally, no zirconium remains among the materials to form $ZrSi_2$. The concurrent formation of $ZrB_2$ and ZrC has also been reported by other researchers [28]. The reduced Si and remaining C may then form SiC as the second carbide phase. These sub-steps may be written as follows:

$Zr + 2B \rightarrow ZrB_2$ (5)

$\Delta G°_{298}= -318$ kJ,  $\Delta H°_{298}= -322$ kJ,  $T_{ad} \approx 3200$ K

$Zr + C \rightarrow ZrC$ (6)

$\Delta G°_{298}= -193$ kJ,  $\Delta H°_{298}= -196$ kJ,  $T_{ad} \approx 3450$ K

$Si + C \rightarrow SiC$ (7)

$\Delta G°_{298}= -70$ kJ,  $\Delta H°_{298}= -73$ kJ,  $T_{ad} \approx 1650$ K

It must be noted that during milling, all the above sub-reactions (equations 3 to 7) occur instantly and simultaneously at the ignition point such that it is impossible to

separate them. In order to examine the proposed mechanism, sub-reactions *(3)* and *(4)* were individually investigated.

Stoichiometric amounts of the starting materials in the $Mg/B_2O_3$ and $Mg/C/ZrSiO_4$ systems were separately mixed according to the reactions *(3)* and *(4)* and were milled under the same conditions. For reaction *(3)*, the ignition time was found to be approximately 8 min (see Fig. 1). The XRD patterns of the initial material and the milled sample up to the ignition point (8 min) are shown in Fig. 5. The ignited sample contains MgO together with trace amounts of the initial remaining Mg due to the entrapment in the dead zones inside the vial, as previously mentioned. Elemental B cannot be observed in the pattern, likely due to its amorphous state because of the extremely high heating and cooling rates during ignition. A small amount of an MgO-rich spinel ($3MgO.B_2O_3$) was also formed after ignition. The formation of this type of spinel phase can be explained as a consequence of a reaction between larger amounts of MgO and smaller amounts of the remaining boron oxide.

For reaction *(4)*, as expected from its thermodynamic data, no pressure rise was observed throughout milling for 4 h. Figure 6 shows the XRD pattern of the un-milled powder and the powder milled for 4 h. Only peak broadening was observed during this period. This result indicates that during milling under the applied conditions, magnesium cannot cause the reaction *(4)* to become self-sustaining to obtain Zr and Si. The products of this reaction might be gradually formed in an ordinary way under more intensive experimental conditions for a much longer time.

Therefore, it can be concluded that the reduction of $B_2O_3$ is the major contributor of the necessary heat to cause the simultaneous reduction of $ZrSiO_4$ and the subsequent formation of the boride and carbide phases.

9

### 3.2.2. Thermal behavior

Differential scanning calorimetry (DSC) was used to study the reaction mechanism during heating. For this purpose, a homogeneously blended $Mg/ZrSiO_4/B_2O_3/C$ powder mixture was subjected to DSC analysis at a heating rate of 10 $^\circ$C/min, as shown in Fig. 7. The DSC curve exhibits two endothermic peaks at approximately 100 °C and 650 °C and two exothermic peaks at approximately 700 °C and 1100 °C. The low–temperature endotherm appears to be related to the vaporization of water adsorbed to the $B_2O_3$. The higher temperature endotherm is related to the melting of magnesium. The reaction between the materials clearly starts with an onset temperature of 700°C, where a sharp and narrow exotherm is observed. The shape of this peak can be a typical sign of a self-sustaining reaction.

Fig. 8 shows the XRD patterns of the products after the heating of the initial mixture at different temperatures, with the aim of clarifying the nature of the peaks appearing in the DSC curve. The XRD pattern corresponding to the annealed sample at 750°C (after the first exotherm in the DSC graph) shows a considerable amount of the MgO phase along with unreacted initial materials. The formation of MgO phase indicates that the first exotherm is related to the reduction of boron oxide by magnesium (reaction *3*). Although the reaction of Mg with $B_2O_3$ is highly exothermic, as shown in Figs. 5 and 7, the experimental conditions used during annealing are insufficient to release enough heat to induce the self-sustaining reduction of zircon and the transformation of all of the reactants into products of reaction *(2)*.

The second exotherm at 1100°C in the DSC curve is broad, ranging from about 950°C to about 1200°C. To clarify the nature of this exotherm, heat treatments were

performed at 1000°C (slightly after start of the exotherm) and 1200°C (the end of the exotherm). The XRD pattern corresponding to the sample heated to 1000°C indicates that a considerable amount of $ZrB_2$ was formed, as shown in Fig. 8. A small amount of magnesium borate ($Mg_2B_2O_5$) and magnesium silicate ($Mg_2SiO_4$) was also formed. The formation of $ZrB_2$ and $Mg_2SiO_4$ demonstrates that the second exotherm is attributed to the decomposition and reduction of $ZrSiO_4$ and the formation of its related products. The XRD results suggest that $ZrSiO_4$ is first decomposed into $ZrO_2$ and $SiO_2$. $ZrO_2$ is subsequently reduced by Mg, and the Zr reacts with B present in the medium to form $ZrB_2$. All the $SiO_2$ transforms to $Mg_2SiO_4$ due to the reaction with MgO prior to the reduction by Mg. Hence, there is no elemental silicon or another compound that includes Si in the XRD pattern. Carbon is observed to remain unreacted among products, and no carbide phase (ZrC or SiC) was formed.

Increasing the temperature to 1200°C causes the $ZrSiO_4$ reduction to be completed with $ZrB_2$ as the major product. However, magnesium silicate and magnesium borate are still present in the system, which account for their stability. Carbon is also present in the system as an unreacted element. The broad shape of the second exotherm in the DSC graph is consistent with the gradual nature of the reduction of zircon. Finally, by increasing the temperature to 1400°C, magnesium borate was dissociated, whereas magnesium silicate was still stable. At this temperature, carbon did not participate in the reaction to form any carbide phase. Contrary to milling experiments, no carbide phases form during the heat treatment, and all of the reduced Zr reacts with boron to form $ZrB_2$. Indeed, the temperature increases gradually in the heating experiments, and these temperatures are insufficient to cause a reaction between Zr and C before the reaction between Zr and B.

11

The annealing treatments described above show evidence for the preliminary reduction of boron oxide, followed by the reduction of zircon at higher temperatures. This general trend is consistent with the mechanism proposed for mechanochemical synthesis. However, since the experimental conditions during the annealing treatments for inducing an SHS process were not met (using loose powder and low heating rate), the differences observed in the final product between milling and annealing routes may be related to the different kinetics associated with self-sustaining and gradual processes. The main difference is the total consumption of $SiO_2$ for the formation of the spinel phase of magnesium silicate in the heat treatments, while $SiO_2$ was mostly reduced to Si in the milling experiments. Before $SiO_2$ could be reduced by Mg during heat treatments, it reacts with MgO to form the silicate phase. The second difference is that carbon did not participate in the reaction to form carbide phases during the heat treatments. Therefore, ordinary heat treatment is not a suitable method to synthesize $ZrB_2$–SiC–ZrC composites.

## 4. Conclusion

High energy ball milling was successfully applied for the mechanosynthesis of a $ZrB_2$–SiC–ZrC composite by means of a magnesiothermic reduction. The synthesis in the $Mg/B_2O_3/ZrSiO_4/C$ system was found to be self-sustaining and to have an ignition time of 6 min of milling. Examination of the sub-reactions revealed that $B_2O_3$ is easily reduced by Mg, while magnesium cannot self-sustain the reduction of $ZrSiO_4$ to Zr and Si. It was concluded that the great deal of heat generated through the reduction of $B_2O_3$ by Mg is capable of activating the reduction of $ZrSiO_4$. It was found that heat treatment

of the $Mg/B_2O_3/ZrSiO_4/C$ system with an ordinary heating rate will not produce the desired composite.

**Acknowledgements**

**References**

[1] W.G. Fahrenholtz, G.E. Hilmas, I.G. Talmy, J.A. Zaykoski, Refractory diborides of zirconium and hafnium, Journal of the American Ceramic Society 90 (2007) 1347–1364.

[2] S.Q. Guo, Densification of $ZrB_2$-based composites and their mechanical and physical properties: A review, Journal of the European Ceramic Society 29 (2009) 995–1011.

[3] S.Q. Guo, J.M. Yang, H. Tanaka, Y. Kagawa, Effect of thermal exposure on strength of $ZrB_2$-based composites with nano-sized SiC particles, Composites Science and Technology 68 (2008) 3033–3040.

[4] F. Monteverde, Beneficial effects of an ultra-fine α-SiC incorporation on the sinterability and mechanical properties of $ZrB_2$, Applied Physics A –Materials Science & Processing 82 (2006) 329–337.

[5] H. Zhang, Y. Yan, Z. Huang, X. Liu, D. Jiang, Properties of $ZrB_2$–SiC ceramics by pressureless sintering, Journal of the American Ceramic Society 92 (2009) 1599–1602.

[6] P. Hu, W. Guolin, Z. Wang, Oxidation mechanism and resistance of $ZrB_2$–SiC composites, Corrosion Science 51 (2009) 2724–2732.

[7] V. Zamora, A.L. Ortiz, F. Guiberteau, M. Nygren, L.L. Shaw, On the crystallite size refinement of $ZrB_2$ by high-energy ball-milling in the presence of SiC, Journal of the European Ceramic Society 31 (2011) 2407–2414.

[8] T. Tsuchida, S. Yamamoto, MA-SHS and SPS of $ZrB_2$–ZrC composites, Solid State Ionics 172 (2004) 215–216.

[9] D. Sciti, F. Monteverde, S. Guicciardi, G. Pezzotti, A. Bellosi, Microstructure and mechanical properties of $ZrB_2$–$MoSi_2$ ceramic composites produced by different sintering techniques, Materials Science and Engineering A 434 (2006) 303–309.

[10] L. Silvestroni, D. Sciti, J. Kling, S. Lauterbach, H.J. Kleebe, Sintering mechanisms of zirconium and hafnium carbides doped with $MoSi_2$, Journal of the American Ceramic Society 92 (2009) 1574–1579.

[11] G. Li, W. Han, X. Zhang, J. Han, S. Meng, Ablation resistance of $ZrB_2$–SiC–AlN ceramic composites, Journal of Alloys and Compounds 479 (2009) 299–302.

[12] J.S. Peters, B.A. Cook, J.L. Harringa, A.M. Russell, Erosion resistance of $TiB_2$–$ZrB_2$ composites, Wear 267 (2009) 136–143.

[13] S.Q. Guo, Y. Kagawa, T. Nishimura, D. Chung, J.M. Yang, Mechanical and physical behavior of spark plasma sintered ZrC–$ZrB_2$–SiC composites, Journal of the European Ceramic Society 28 (2008) 1279–1285.

[14] A. Snyder, D. Quach, J.R. Groza, T. Fisher, S. Hodson, L.A. Stanciu, Spark Plasma Sintering of $ZrB_2$–SiC–ZrC ultra-high temperature ceramics at 1800°C, Materials Science and Engineering A 528 (2011) 6079–6082.

[15] Q. Qiang, H. Jiecai, H. Wenbo, Z. Xinghong, H. Changqing, In situ synthesis mechanism and characterization of $ZrB_2$–$ZrC$–$SiC$ ultra high-temperature ceramics, Materials Chemistry and Physics 110 (2008) 216–221.

[16] W.W. Wu, G.J. Zhang, Y.M. Kan, P.L. Wang, Reactive Hot Pressing of $ZrB_2$–$SiC$–$ZrC$ Composites at 1600°C, Journal of the American Ceramic Society 91 (2008) 2501–2508.

[17] A.K. Khanra, L.C. Pathak, S.K. Mishra, M.M. Godkhindi, Sintering of ultrafine zirconium diboride powder prepared by modified SHS technique, Advances in Applied Ceramics 104 (2005) 282–284.

[18] K. Nishiyama, T. Nakamur, S. Utsumi, H. Sakai, M. Abe, Preparation of ultrafine boride powders by metallothermic reduction method, Journal of Physics: Conference Series 176 (2009) 012043.

[19] N. Setoudeh, N.J. Welham, Formation of zirconium diboride ($ZrB_2$) by room temperature mechanochemical reaction between $ZrO_2$, $B_2O_3$ and Mg, Journal of Alloys and Compounds 420 (2006) 225–228.

[20] S.K. Mishra, S. Das, L.C. Pathak, Defect structures in zirconium diboride powder prepared by self-propagating high-temperature synthesis, Materials Science and Engineering A364 (2004) 249–255.

[21] B. Akgun, H.E. Camurlu, Y. Topkaya, N. Sevinc, Mechanochemical and volume combustion synthesis of $ZrB_2$, International Journal of Refractory Metals and Hard Materials 29 (2011) 601–607.

[22] Y.B. Lee, H.C. Park, K.D. Oh, C.R. Bowen, R. Stevens, Self-propagating high-temperature synthesis of $ZrB_2$ in the system $ZrO_2$-$B_2O_3$-$Fe_2O_3$-Al, Journal of Materials Science Letters 19 (2000) 469– 471.

[23] F.J. Gotor, M. Achimovicova, C. Real, P. Balaz, Influence of the milling parameters on the mechanical work intensity in planetary mills, Powder Technology 233 (2013) 1–7.

[24] www.factsage.com

[25] Z.A. Munir, U. Anselmi-Tamburini, Self-propagating exothermic reactions: The synthesis of high-temperature materials by combustion, Materials Science Reports 3 (1989) 277-365.

[26] M. Jalaly, M.Sh. Bafghi, M. Tamizifar, F. J. Gotor, Mechanosynthesis of nanocrystalline $ZrB_2$- based powders by mechanically induced self-sustaining reaction method, Advances in Applied Ceramics, 112 (2013) 383-388.

[27] L. Takacs, Self-sustaining reactions induced by ball milling, Progress in Materials Science 47 (2002) 355–414.

[28] H. Y. Ryu, H.H. Nersisyan, J.H. Lee, Preparation of zirconium-based ceramic and composite fine-grained powders, International Journal of Refractory Metals and Hard Materials 30 (2012) 133–138.
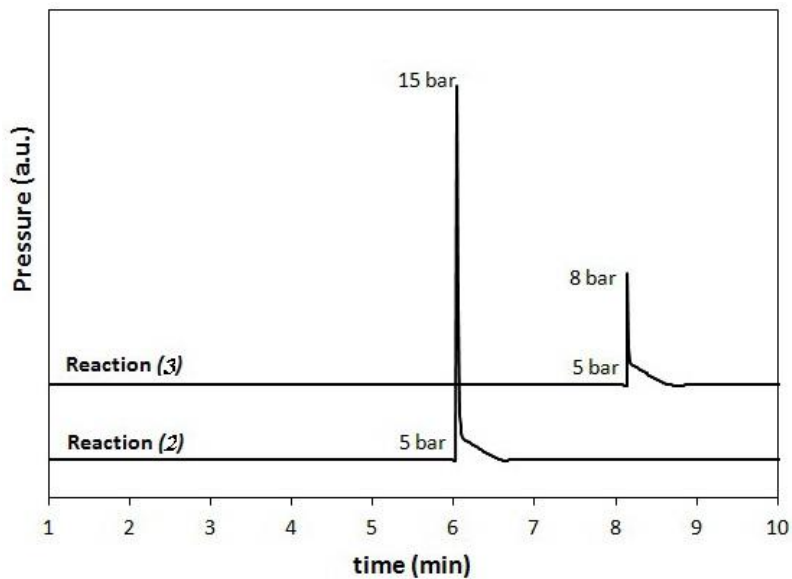
Fig. 1. Pressure inside the vial versus milling time for the $Mg/ZrSiO_4/B_2O_3/C$ (reaction 2) and $Mg/B_2O_3$ (reaction 3) systems.

16
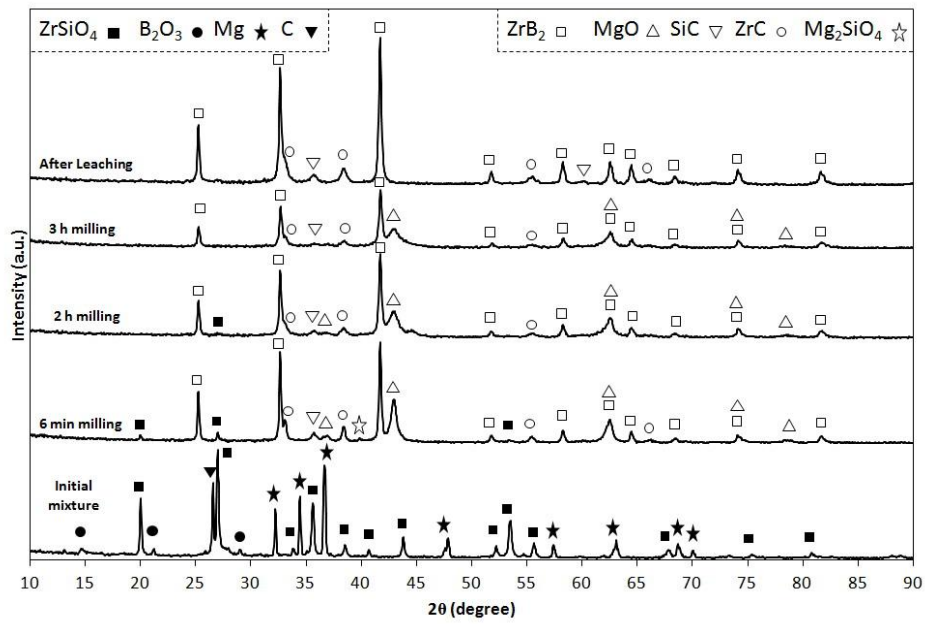
Fig. 2. X-ray diffraction patterns of the as-blended, milled and leached samples of the

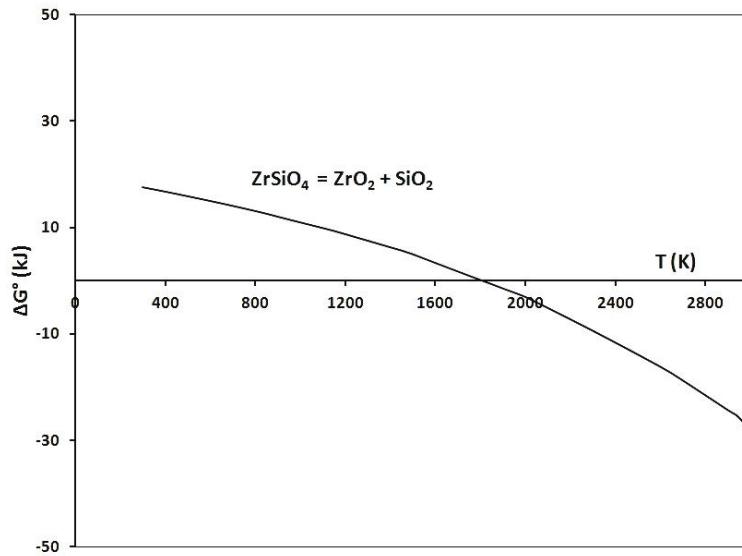Mg/ZrSiO$_4$/B$_2$O$_3$/C system.



Fig. 3. Standard free energy of zircon decomposition to its individual oxides versus temperature.
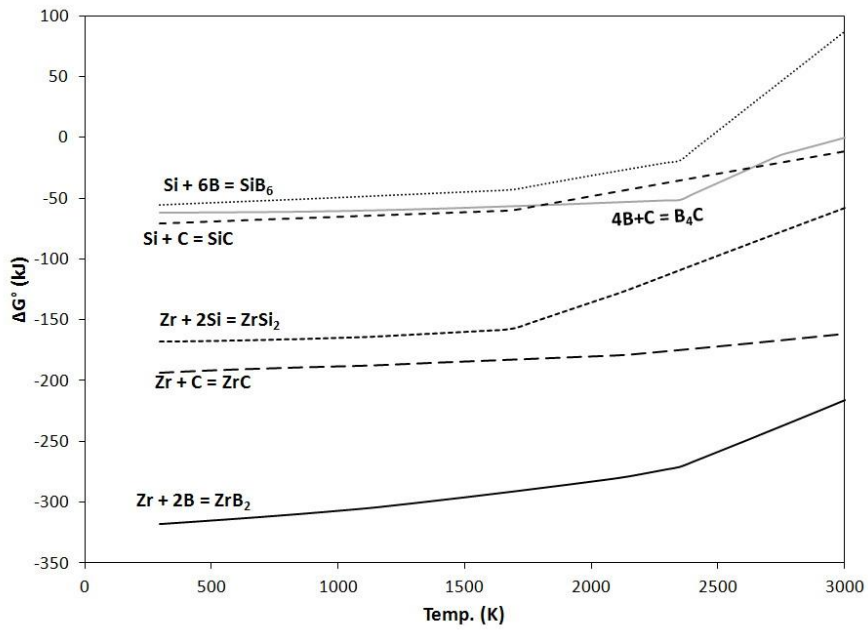
Fig. 4. Standard free energy of formation for various potential compounds capable of
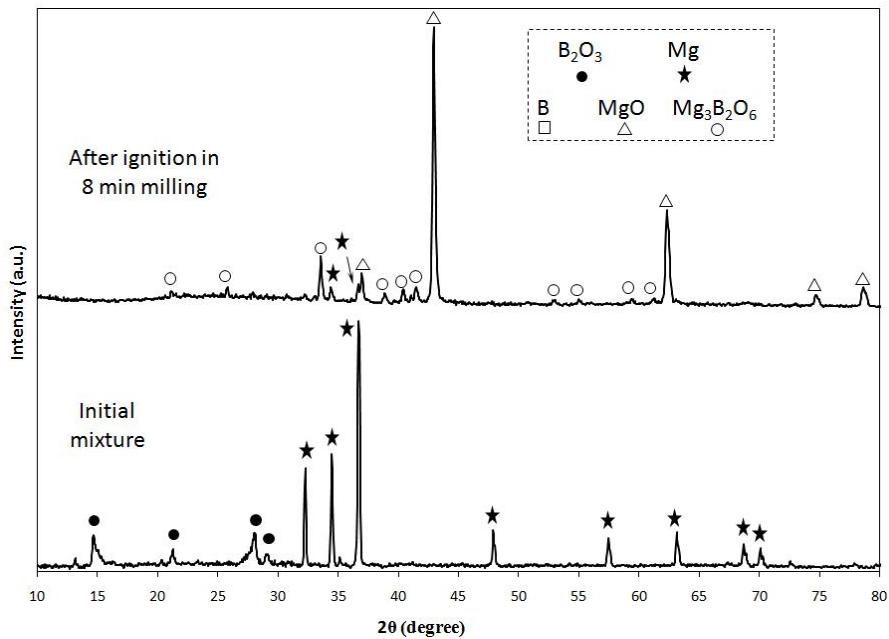
being created from elemental Zr, Si, B and C.



Fig. 5. X-ray diffraction patterns of the initial and milled samples of the $Mg/B_2O_3$ system.
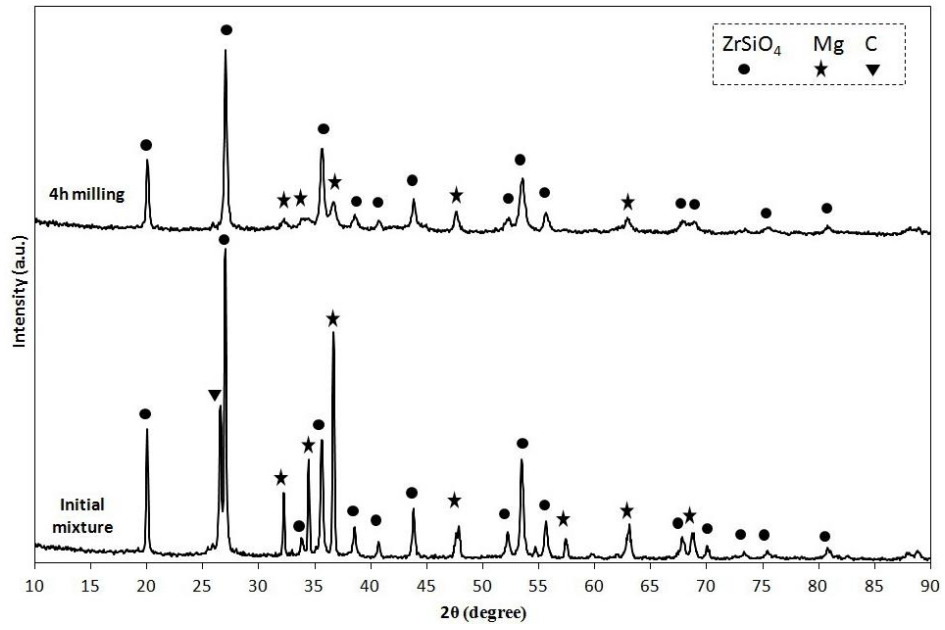
Fig. 6. X-ray diffraction patterns of the initial and milled samples of the Mg/ZrSiO$_4$/C system.
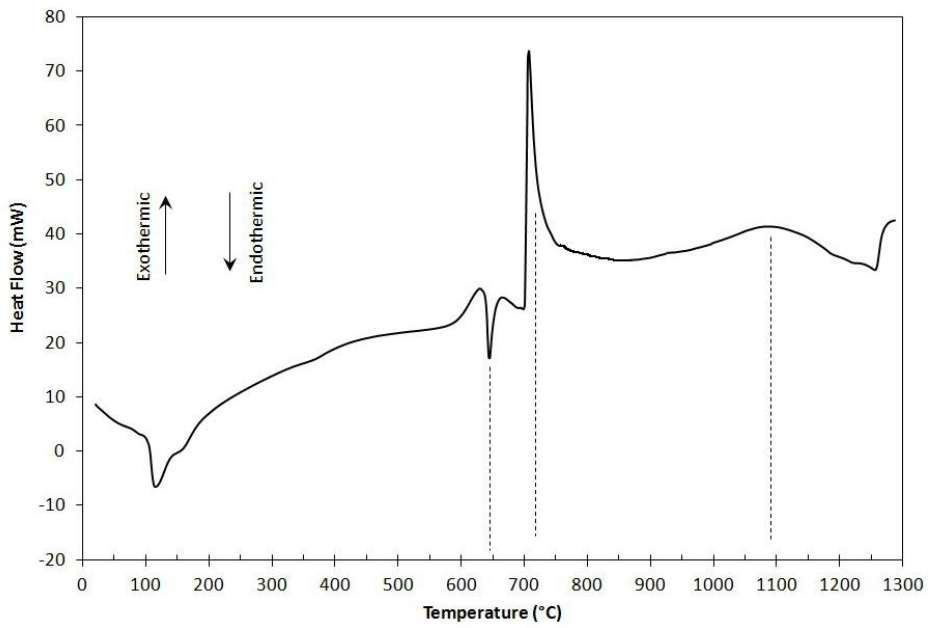


Fig. 7. DSC curve of the as-blended mixture in the Mg/ZrSiO$_4$/B$_2$O$_3$/C system.
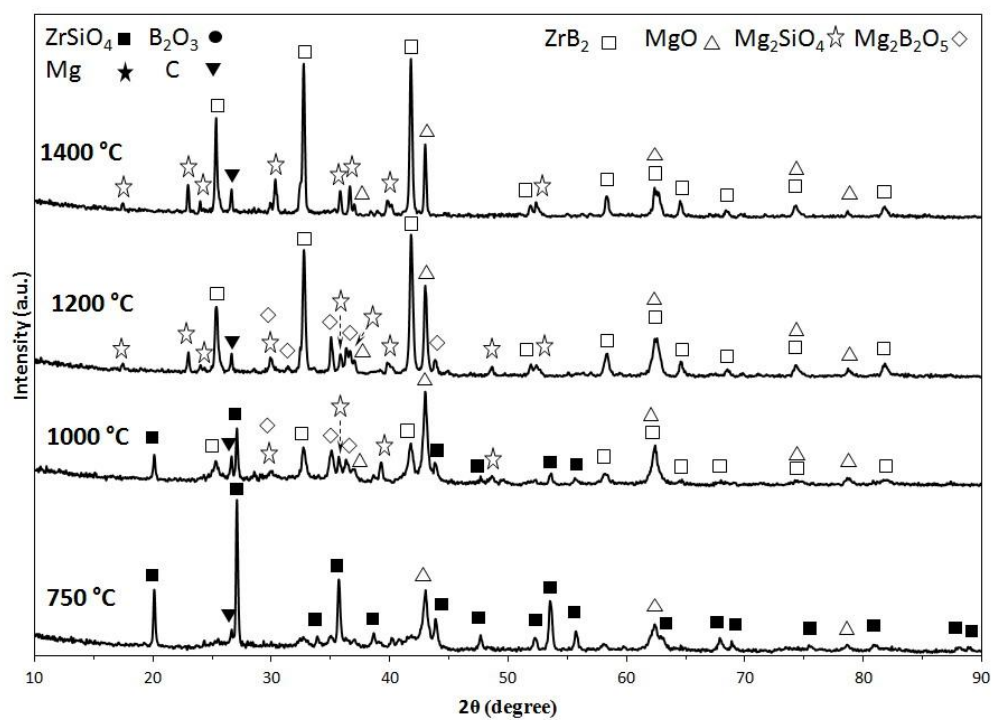
Fig. 8. X-ray diffraction patterns of the blended powders in the Mg/ZrSiO$_4$/B$_2$O$_3$/C system after heating at 750, 1000, 1200 and 1400°C (30 min dwell time at maximum temperature prior to cooling inside the furnace to room temperature).